

MODEL OF FRACTIONATION AND COALESCENCE OF GAS BUBBLES IN A TURBULENT LIQUID FLOW

V. A. Sosinovich, V. A. Tsyganov,
B. I. Puris, and V. A. Gertsovich

UDC 532.529.6

A system of equations for describing the evolution of the size range of gas bubbles as a result of their fractionation and coalescence in an isotropic turbulent decaying flow of incompressible liquid is derived and solved numerically. Outer parameters are found by which one can effectively control the probability distribution of the bubble radii.

An equation for describing the evolution of gas bubbles in a turbulent liquid flow was derived and solved in [1]. Here, only the process of turbulent fractionation of bubbles was taken into account. The present study is aimed at the development of a model which could allow for both fractionation and coalescence of bubbles in a turbulent flow of incompressible liquid. The account for the coalescence process makes it possible to allow for the effect of gas saturation.

1. Equation for $f_1(r)$ Describing the Process of Gas Bubble Coalescence in a Turbulent Flow. As a main object of investigation we take the probability density distribution of bubble radii $f_1(r)$. The function $N(t)$, the quantity of bubbles per unit volume of a gas-liquid system, i.e., the concentration of bubbles, is necessary for the further presentation. This can be calculated by formula (8) from [1].

We first write the equation for the function $f_1(r)$ for the case of coalescence only, in the absence of fractionation. The complete equation for $f_1(r)$ with allowance for both coalescence and fractionation can be then found by adding the right side of the equation describing the process of turbulent fractionation to the right side of the obtained equation. As a basis we use the Smolukhovskii-Müller equation for the function $\varphi(v, t)$, which gives the distribution of coagulating particles over volumes v [2]:

$$\frac{\partial \varphi(v, t)}{\partial t} = \frac{1}{2} \int_0^v \beta(v, v_1) \varphi(v - v_1, t) \varphi(v_1, t) dv_1 - \varphi(v, t) \int_0^\infty \beta(v, v_1) \varphi(v_1, t) dv_1. \quad (1)$$

Here $\beta(v_1, v_2)$ is the frequency of pair collisions of bubbles with volumes v_1 and v_2 . The function $\varphi(v, t)$ is defined so that the integral with respect to the variable v of this function gives the total number of particles per unit volume of the gas-liquid system

$$\int_0^\infty \varphi(v, t) dv = N(t). \quad (2)$$

Integrating (1) with respect to the volume, we obtain the equation for the concentration of bubbles $N(t)$

$$\frac{dN(t)}{dt} = \frac{1}{2} \int_0^\infty \int_0^\infty \beta(v_1, v_2) \varphi(v_1, t) \varphi(v_2, t) dv_1 dv_2. \quad (3)$$

We determine the function $\psi(v, t)$ by the formula

$$\psi(v, t) = \frac{\varphi(v, t)}{N(t)}. \quad (4)$$

We can see from (2) and (4) that this formula is normalized to unity. Using (4) we can write the equality

$$\frac{\partial \psi(v, t)}{\partial t} = \frac{1}{N(t)} \frac{\partial \varphi(v, t)}{\partial t} - \frac{\varphi(v, t)}{N^2(t)} \frac{dN(t)}{dt}. \quad (5)$$

Having replaced $\partial \varphi(v, t) / \partial t$ by the right side of equation (1) and replaced $\varphi(v, t)$ by $\psi(v, t)$ according to formula (4), we obtain the equation

$$\begin{aligned} \frac{\partial \psi(v, t)}{\partial t} = N(t) & \left\{ \frac{1}{2} \int_0^v \beta(v - v_1, v_1) \psi(v - v_1, t) \psi(v_1, t) dv_1 - \right. \\ & \left. - \psi(v, t) \int_0^\infty \beta(v, v_1) \psi(v_1, t) dv_1 \right\} - \frac{\psi(v, t)}{N(t)} \frac{dN(t)}{dt}. \end{aligned} \quad (6)$$

To pass over to the variable r we use the obvious relations

$$\psi(v, t) dv = f_1(r) dr, \quad f_1(r) = \psi(v, t) \frac{dv}{dr}, \quad v = \frac{4}{3} \pi r^3. \quad (7)$$

Then the equation for $f_1(r)$ – the probability density of bubble radii – will have the form [3]

$$\begin{aligned} \frac{\partial f_1(r)}{\partial t} = N(t) & \left\{ \frac{1}{2} \int_0^r \frac{r^2}{(r^3 - r_1^3)^{2/3}} \beta[(r^3 - r_1^3), r_1^3] f_1[(r^3 - r_1^3)^{1/3}] \times \right. \\ & \left. \times f_1(r_1) dr_1 - f_1(r) \int_0^\infty \beta(r^3, r_1^3) f_1(r_1) dr_1 \right\} - \frac{f_1(r)}{N(t)} \frac{dN(t)}{dt}. \end{aligned} \quad (8)$$

All forms of the Smolukhovskii–Müller equation involve the function $\beta(r_1^3, r_2^3)$, the meaning of which is the frequency of pair collisions of bubbles with volumes v_1 and v_2 . The problem is to write an implicit form of this function for the case of coalescence of bubbles in a turbulent liquid flow. As was shown in [4], the coefficient of bubble diffusion in a turbulent liquid flow due to turbulence for bubbles of radius $r > (10^{-7} - 10^{-8})$ m is much higher than the coefficient of diffusion due to Brownian motion. Since the minimum bubble radius as a result of turbulent fractionation at Reynolds numbers $Re \sim 10^4$ (characteristic scale 10^{-3} m, kinematic viscosity 10^{-6} m²/sec) is about 10^{-5} m, then the contribution of Brownian motion to the coefficient of bubble diffusion can be neglected, and only turbulent diffusion is taken into account.

An analogy between turbulent and Brownian diffusion [5] makes it possible to write an expression for the function $\beta(r_1^3, r_2^3)$ in the following form:

$$\beta(r_1^3, r_2^3) = 4\pi [D_{\text{tur}}(r_1, t) + D_{\text{tur}}(r_2, t)] (r_1 + r_2), \quad (9)$$

where $D_{\text{tur}}(r, t)$ is the differential coefficient of turbulent diffusion related to the energy distribution of turbulent fluctuations over different length scales. As was suggested in [6] on deriving a closed equation for $P_1(r)$, this quantity can be related to $P_1(r)$ by the formula

$$D_{\text{tur}}(r, t) = \delta \int_r^\infty [P_1(\tilde{r}) \tilde{r}]^{1/2} d\tilde{r}, \quad (10)$$

which shows that $D_{\text{tur}}(r, t)$ allows only for fluctuations with length scales exceeding the bubble radius. Fluctuations of smaller length scales result only in bubble deformation, but not in diffusion. The factor δ in (10) allows for the

excess of the coefficient of turbulent diffusion of gas bubbles in the liquid over the coefficient of turbulent diffusion of liquid particles of the carrying flow that is caused by the difference in densities of the liquid and the gas in a bubble. As shown in [7], at a small bubble size the factor can reach the value $\delta \approx 4.5$.

Thus, Eqs. (9), (10) give the function $\beta(r_1^3, r_2^3)$ in terms of the distribution of turbulent energy over different length scales.

2. Equation for $f_t(t)$ Evolution with Allowance for Processes of Coalescence and Fractionation of Gas Bubbles. In a gas-liquid turbulent flow the processes of fractionation and coalescence of gas bubbles occur simultaneously with one of them being predominant, depending on the size of bubbles and various turbulent parameters. Fractionation of bubbles takes place only when the intensity of turbulent fluctuations of velocity exceeds a certain threshold value, which is different for different bubble sizes, i.e., for a turbulent field of fixed strength there exists a certain critical bubble size such that bubbles with a radius greater than critical fractionate. An equation describing the process of bubble fractionation in a turbulent flow is derived in [1], and it is determined by formula (28).

A complete equation with allowance for both coalescence and fractionation can be obtained by combining the right-hand sides of Eq. (8) of the present work and Eq. (28) from [1]. We write this resultant equation in dimensionless variables employing the notation from [1]:

$$\begin{aligned} \frac{\partial f_t(r)}{\partial t} = N(t) & \left\{ \frac{1}{2} \int_0^r \frac{r^2}{(r^3 - r_1^3)^{3/2}} \beta[(r^3 - r_1^3), r_1^3] f_t[(r^3 - r_1^3)^{1/3}] \times \right. \\ & \left. \times f_t(r_1) dr_1 - f_t(r) \int_0^\infty \beta(r^3, r_1^3) f_t(r_1) dr_1 \right\} - \frac{f_t(r)}{N(t)} \frac{dN(t)}{dt} - \\ & - \frac{f_t(r)}{\tau(r)} \theta[r - a_{cr}(t)] + \int_r^\infty \frac{f_t(r)}{\tau(r)} \omega(r, R) dR. \end{aligned} \quad (11)$$

The function $N(t)$ can be calculated from Eq. (8) of [1] using a value of gas saturation α chosen within the range (0-1). The quantity $a_{cr}(t)$ is calculated by Eq. (15) of [1]. The derivation of the relation for $\tau(R)$ was based in [1] on the employment of the criterion according to which the actual Weber number should be larger than some critical value [8, 9]. The assumption that the velocity of the disturbance of a bubble surface is less than the sound velocity in the liquid c yields the following formula for $\tau(R)$:

$$\tau(r) = \frac{k_1 \left[\frac{\lambda(t)}{\lambda(2R, t)} \right] + 2Rk_2 B(t)^{3/2}}{B(2R, t)^{3/2}}, \quad (12)$$

where

$$\lambda(2R, t) = \int_0^{2R} r P_1(r) dr / B(2R, r), \quad \lambda(t) = \int_0^\infty r P_1(r) dr / B(t); \quad (13)$$

$$B(2R, t) = \int_0^{2R} P_1(r) dr, \quad B(t) = \int_0^\infty P_1(r) dr; \quad (14)$$

$$k_1 = \frac{2r_0}{L We} (6/k_f)^{1/2} (\rho'/\rho)^{1/2}, \quad We = \frac{2r_0 \rho' B(0)}{\sigma}, \quad k_2 = \frac{B(0)^{1/2}}{c}. \quad (15)$$

The function $P_1(r)$ necessary for calculations is calculated from the closed equation

$$\frac{\partial P_1(r)}{\partial t} = \frac{\partial}{\partial r} \left\{ \left[\frac{2}{\text{Re}} + 2\gamma \int_0^r [\tilde{r} P_1(\tilde{r})]^{1/2} d\tilde{r} \right] \left(\frac{\partial}{\partial r} + \frac{4}{r} \right) P_1(r) \right\}, \quad (16)$$

where $\gamma = 0.24$; $\text{Re} = LB(0)^{1/2}\nu$ is the Reynolds number, where L is the initial scale of the velocity fluctuation field; ν is the kinematic viscosity of liquid. The initial and boundary conditions for the function $P_1(r)$ have the form

$$P_0(r) = 2r \exp(-r^2); \quad P_1(0) = P_1(\infty) = 0. \quad (17)$$

The expression for the function $\omega(r, R)$, which specifies the mode of bubble fractionation, is written as formulas (30), (31), (33), (34) in [1]. The initial condition for $f_1(r)$ can be represented in the form of the parabola

$$f_0(r) = -\frac{3(r-r_0)^2}{4\Delta^3} + \frac{3}{4\Delta}. \quad (18)$$

The system of equations (10), (16) was solved by the implicit finite-difference technique in combination with an iteration process for nonlinearities. The initial condition for $f_1(r)$ was assigned in the form of (18). The initial condition for $P_1(r)$ was chosen in the form of (17). The sweep method was used to solve the equation for $P_1(r)$. The mesh of the space grid increased with r . The convergence of the iterations at each time step was estimated by the quantities $|(P_s - P_{s+1})/(P_s + P_{s+1})| < 10^{-5}$; $|(f_s - f_{s+1})/(f_s + f_{s+1})| < 10^{-4}$, where P_s and f_s are the values of the functions $P_1(r)$ and $f_1(r)$ in iteration s .

3. Results of the Numerical Solution of the System of Equations for $f_1(r)$ with Allowance for Coalescence and Fractionation. Before starting the discussion of the results of numerical calculation we shall make the following explanation. In the present study an attempt is made to simulate, using the language of isotropic turbulence, the situation which is realized in a cavitation module for gas dispersion in a liquid with subsequent fractionation of bubbles in a turbulent liquid flow and their coalescence. In a real cavitation unit, the liquid flow passes through a plane with a sudden cross-section expansion, is mixed with air, and acquires a larger turbulent energy. As the gas-liquid flow moves further, turbulent energy decreases due to dissipation, but since the flow moves in a channel there simultaneously take place constant generation of turbulent energy near the walls and its diffusion over the entire volume of the flow. As a result, the channel cross-section-mean turbulent energy is fixed at the level characteristic of the channel flow. In the interior of the turbulent liquid along the entire path of the cavitation unit there occur fractionation and coalescence of gas bubbles formed due to cavitation saturation in the plane where the flow suddenly expanded. As a result, at the outlet from the cavitation unit there exists a gas-liquid flow with some size distribution of bubbles and a certain concentration of them that depends on the specific conditions in the turbulent flow.

The described pattern is simulated by the following calculation. At the instant $t = 0$, the initial distribution of turbulent energy is specified in the liquid over a different length scale $P_0(r)$. Its parameters (energy and mean length scale) are selected so that it reproduces the situation in the section of sudden flow expansion. Then this distribution develops according to Eq. (16) until the energy attains the value characteristic of turbulence in the channel. Then, the function $P_1(r)$ is considered stationary with a fixed energy level. $P_1(r)$ was calculated without regard for the presence of bubbles in the liquid. Results of the calculation are given below in dimensionless form with the following characteristic dimensions: $r_c = 10^{-3}$ m, $B_c(0) = 100$ m²/sec², $f_c = 1/r_c$, $\omega_c = 1/r_c$, $P_c = B_c(0)/r_c$, $t_c = r_c/B_c(0)^{1/2}$, $N_c = 1/r_c^3$. The distribution of probabilities of bubble radii $f_1(r)$ that is formed due to cavitation gas saturation is specified at the initial time instant. The evolution of $f_1(r)$ is calculated in accordance with the above equation (11) on the basis of first decaying and then stationary turbulent flow in the liquid.

Figure 1 presents the evolution of the function of the probability distribution of bubble radii $f_1(r)$ at different values of the mean initial bubble radius. The initial distribution is assigned according to Eq. (18) at $r_0 = 1$ and $r_0 = 2$. It is seen from Fig. 1 that evolution of the function $f_1(r)$ under the effect of the turbulent velocity field is in a shift towards smaller sizes of bubbles. When $t \approx 4$ a reverse shift of the distribution to the right, toward larger sizes, starts. The process of fractionation without regard for coalescence, as was shown in [1], terminated when

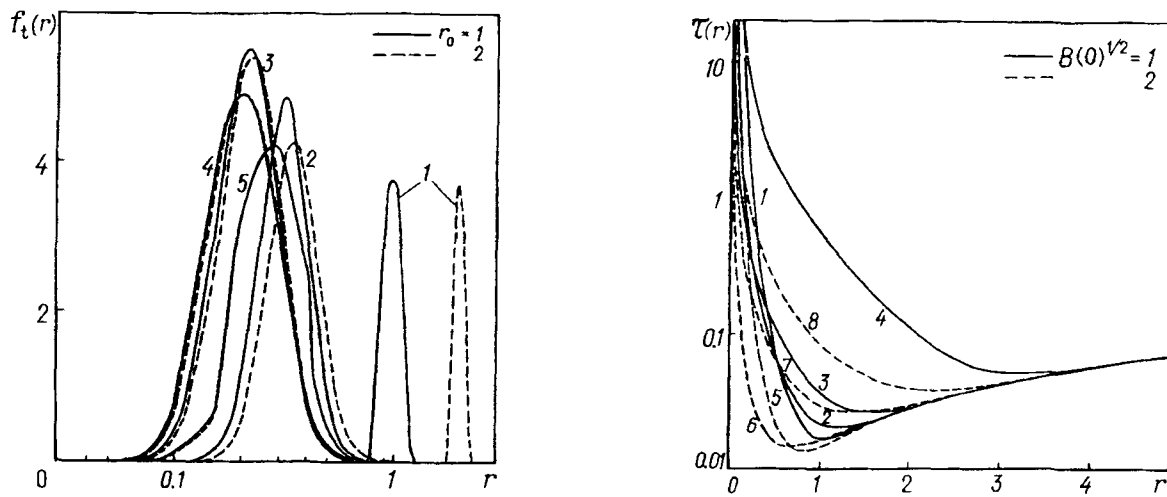


Fig. 1. Evolution of $f_t(r)$ for different initial bubble radii: 1) $t = 0$, 2) 0.3, 3) 1.0, 4) 4.0, 5) 15.0.

Fig. 2. Characteristic time of bubble fractionation as a function of radius: 1, 5) $t = 0$; 2, 6) 0.3, 3, 7) 1.0; 4, 8) 4.0.

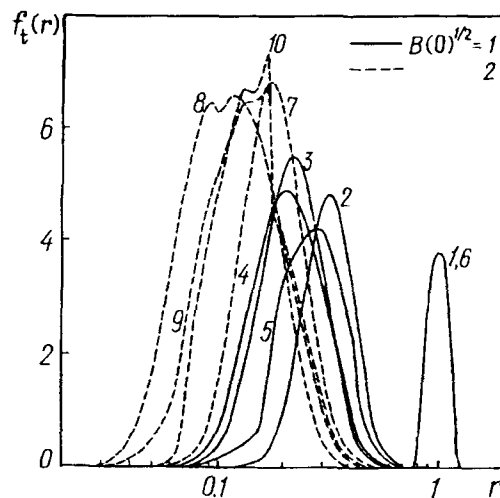


Fig. 3. Evolution of $f_t(r)$ for different initial levels of turbulent energy: 1, 6) $t = 0$; 2, 7) 0.3; 3, 8) 1.0; 4, 9) 4.0; 5, 10) 15.0.

$t \approx 1.25$. In the presence of coalescence this process is prolonged. Minimum mean sizes of bubbles are attained at $t = 2$. As in the absence of coalescence, the dependence of the time required to establish a final distribution on the initial bubble size is weak. It is seen from Fig. 1 that when $t \geq 4$ the dependence of the form of the function $f_t(r)$ on the initial bubble size r_0 vanishes completely. This is also confirmed by results of calculation of the mean radius and dispersion of the bubbles. This insensitivity to the initial bubble size is explained by the fact that the characteristic time of fractionation $\tau(r)$ increases greatly with a decrease in the radius. It is seen from the plots for $\tau(r)$ in Fig. 2 that for bubbles of sizes smaller than $r = 1$, the time of fractionation increases substantially. Such a strong dependence of $\tau(r)$ on the radius results in the fact that large bubbles fractionate more quickly and, finally, the functions $f_t(r)$, being at first different, become equal.

The noted peculiarity of the dependence of the characteristic time of fractionation on size results in insensitivity of the final form of $f_t(r)$ to the initial form. This statement is illustrated by the results of calculation of $f_t(r)$ at different values of Δ given in Fig. 5 of [1]. It is seen that by $t = 0.3$ any difference between initially different distributions $f_t(r)$ disappears. This insensitivity to the initial form of $f_0(r)$ is also confirmed by the results of calculation of bubble concentration $N(t)$.

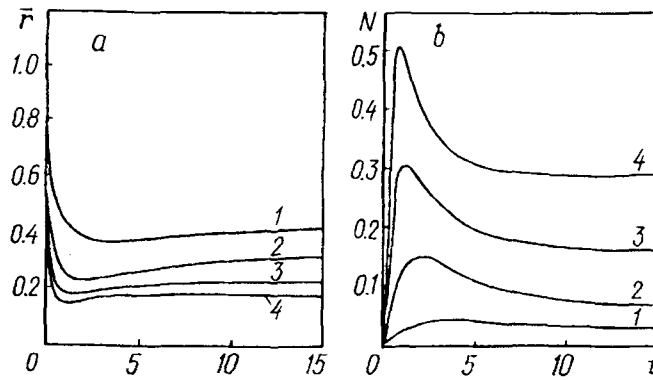


Fig. 4. Evolution of mean radius (a) and concentration (b) of bubbles at different levels of turbulent energy: 1) $B(0)^{1/2} = 0.5$; 2) 1.0; 3) 1.5; 4) 2.0.

Thus, the mean initial size of bubbles and the dispersion of the distribution turn out to be insignificant parameters for controlling the size-distribution of bubbles at the outlet of the unit in which coalescence and fractionation of bubbles occur. The same conclusion was made in [1], where only the process of turbulent fractionation was taken into account.

A much more effective means of controlling the probability distribution of bubble sizes is variation of the turbulence parameters. Figure 3 shows the evolution of the function $f_1(r)$ calculated at different initial levels of turbulent energy with a constant scale of the length of the turbulent velocity field. It is seen from the figure that at larger values of turbulent energy the process of bubble fractionation is more intense. This is in correspondence with the dependence of the characteristic time of fractionation on the turbulence intensity (Fig. 2). In contrast to the case of the absence of coalescence [1] a reverse motion of $f_1(r)$ toward larger bubble sizes caused by bubble coalescence is observed (see curves 9, 10, and 4, 5 in Fig. 3).

Figure 4 presents the time variation of the mean bubble radius for different levels of initial turbulent energy. It is seen that the increase in the mean bubble radius starts earlier in the case of larger values of initial turbulent energy. The growth of $r(t)$ under the effect of coalescence does not lead to a noticeable convergence of curves corresponding to different values of $B(0)$ even at larger times, i.e., the achieved difference in the distribution at the beginning of the fractionation process appears to be stable. At $B(0)^{1/2} = 2$ the mean bubble radius turns to be smaller by a factor of 2.5 than at $B(0)^{1/2} = 0.5$ (see Fig. 4a).

Figure 4b shows the evolution of the concentration as a function of different initial levels of turbulent energy with a constant initial scale L . It is seen that the higher the initial level of turbulence, the higher the bubble concentration. This is caused by the enhancement of the process of turbulent fractionation of bubbles in a flow with higher turbulent energy. The maximum of $N(t)$ at small times is explained by the predominance of the fractionation process at the beginning. When turbulence becomes weaker the concentration of bubbles starts to decrease due to coalescence. As is seen from Fig. 4b with a twofold increase in the initial value of the mean-square fluctuations the final bubble concentration increases by a factor of 3.5. It follows from the presented results that variation of the energy of a turbulent flow is an effective means for controlling the size distribution and concentration of bubbles.

A change in the characteristics of the bubble distribution can also be achieved by variation of the initial length scale L . The time variation of the characteristics of the turbulent velocity field in the background of which the evolution of the probability distribution of bubble radii occurs is in the following. The evolution of the distribution of turbulent energy over the length scale $P_1(r)$ at different initial scales L is realized in a similar way. First, fractionation of turbulent eddies results in a shift of the distribution $P_1(r)$ to the region of smaller length scales. On the termination of the nonequilibrium period, decay of the spectrum is observed with a slight shift of the spectrum maximum to the right. Attenuation of the intensity of turbulent fluctuations from the maximum to a stable value is noticeably slowed with an increase in the initial value of the length scale. The dissipation rate at the maximum for small L substantially exceeds that for large L .

The mentioned turbulent characteristics with a change in the initial length scale determine the corresponding variation of parameters directly affecting evolution of the probability distribution of gas bubble radii.

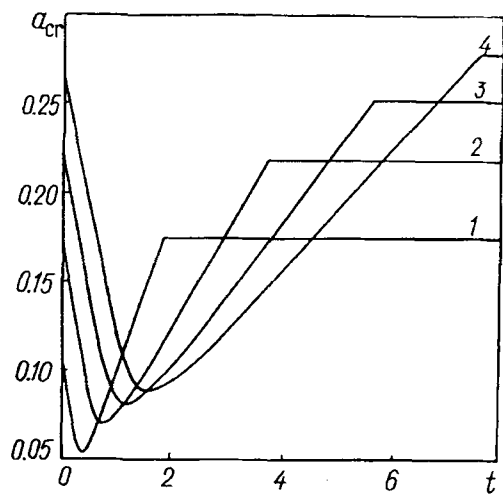


Fig. 5. Evolution of bubble critical radius at different initial scales of the length of the turbulent velocity field: 1) $L = 0.5$; 2) 1.0; 3) 1.5; 4) 2.0.

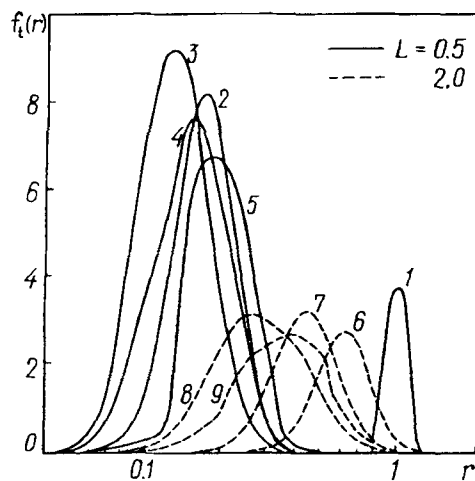


Fig. 6. Evolution of $f_t(r)$ for different initial scales of the length of the turbulent velocity field: 1) $t = 0$; 2, 6) 0.3; 3, 7) 1.0; 4, 8) 4.0; 5, 9) 15.0.

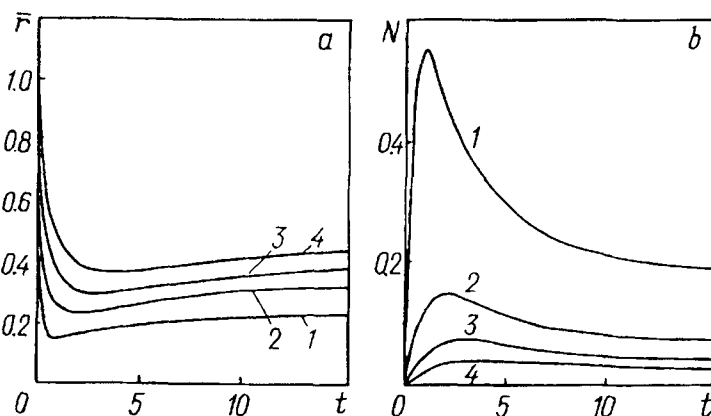


Fig. 7. Evolution of mean radius (a) and concentration (b) of bubbles for different initial scales of the length of the turbulent velocity field: 1) $L = 0.5$; 2) 1.0; 3) 1.5; 4) 2.0.

Figure 5 shows the dependence of the evolution of bubble critical radius on L . It is seen that in a small-scale turbulent velocity field the critical values of bubble radii are much smaller than in a turbulent field with a greater value of L . The intensity of fractionation, which is determined by $\tau(r)$, greatly depends on the length scale L .

A comparison of the evolution of the function of the probability distribution $f_t(r)$ for $L = 0.5$ and $L = 2$ shows that the final size distributions of bubbles (curves 5 and 9 in Fig. 6) remain substantially different. The mean radii of the bubbles (Fig. 7a) differ by about twofold and the maximum radii by about 2.2 times for $L = 0.5$ and $L = 2$. The dependence of the mean radius on time has two characteristic regions (Fig. 7a). The first describes fast reduction in bubble sizes and is associated with fractionation in an intense turbulent field of liquid velocity, and the second shows a gradual increase in bubble sizes due to coalescence. In the absence of coalescence [1] the second region is represented by a straight line. Dispersion of bubble sizes in the region of fractionation decreases, whereas in the region of coalescence it slowly grows. Figure 7b presents the change of concentration with time at different values of the initial scale of turbulence length. It is seen from the plots that the mean concentration of bubbles $N(t)$ can be controlled within a wide range by varying L . The final values of $N(t)$ for the cases of $L = 0.5$ and $L = 2$ differ by 10 times.

It follows from the effect of the initial length scale of the turbulent velocity field on the characteristics of a gas-liquid system that the variation of L is an effective means for controlling the probability distribution of bubble

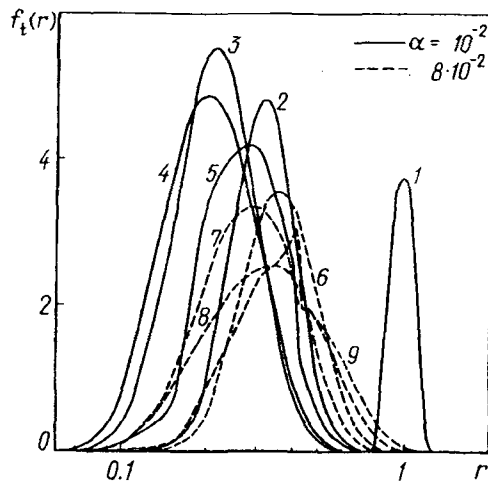


Fig. 8. Evolution of $f_t(r)$ at different values of gas content in liquid: 1) $t = 0$; 2, 6) 0.3; 3, 7) 1.0; 4, 8) 4.0; 5, 9) 15.0.

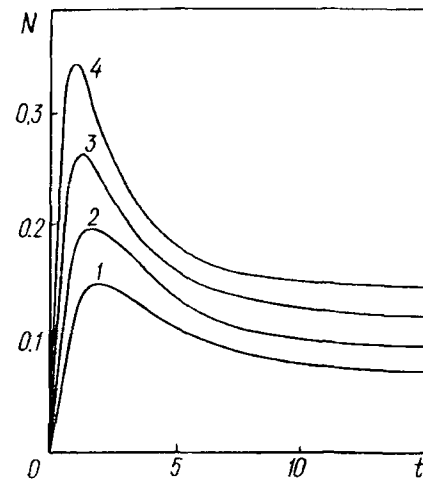


Fig. 9. Evolution of bubble concentration at different values of gas content in liquid: 1) $\alpha = 10^{-2}$; 2) $2 \cdot 10^{-2}$; 3) $4 \cdot 10^{-2}$; 4) $8 \cdot 10^{-2}$.

sizes. The dependences of the steady-state values of the mean radius r and concentration N on the length scale L confirm the above statement.

One more means for controlling the characteristics of the probability distribution of bubble sizes is variation of the gas content of the flow. Figure 8 presents the evolution of the probability density of bubble radii $f_t(r)$ calculated at two values of volume gas concentration α . The mean and maximum radii of bubbles are much smaller at a smaller gas content. The values of distribution dispersion at different α differ greatly. Large dispersions correspond to larger gas contents, which is seen from the evolution curves of $f_t(r)$ at different values of α . As is seen from Fig. 8, this dependence of $f_t(r)$ on gas content is associated with the fact that in the case of a larger gas content the process of coalescence, which competes with the process of bubble fractionation, begins at early stages of gas system evolution. Therefore, bubble sizes at the steady state are much larger. Blurring of the distribution is caused, as in other cases, by large bubble sizes.

Figure 9 presents the dependence of the concentration of bubbles in gas saturation. It is seen that the difference in concentration acquired at the fractionation stage remains at the steady-state stage of the evaluation of a gas-liquid system.

Thus, the size distribution and concentration of bubbles can be controlled by gas content.

CONCLUSIONS

A system of equations describing coalescence and fractionation of bubbles in a turbulent flow of incompressible fluid is obtained and studied numerically. The function of probability density distribution of bubble radii $f_t(r)$, changing with time, is calculated by an equation in which variable quantities such as the frequency of pair collisions of bubbles, critical radius, and characteristic time of bubble fractionation are found by the function of turbulent energy distribution over the length scales.

The obtained system of equations was calculated for different initial distributions of bubble radii, the initial intensity and characteristic scale of the turbulent velocity field, and the gas content.

The following regularities were found as a result of calculations:

1) The evolution of the function $f_t(r)$ under the effect of a turbulent velocity field is reduced first to a shift to small bubble radii, which is caused by intense fractionation of bubbles in the turbulent liquid flow, and then to a slow shift toward larger bubble radii under the effect of coalescence.

2) The final stationary function $f_t(r)$ and the time of its establishment weakly depend on the mean bubble size in the initial distribution and are practically not determined by the dispersion of the initial distribution.

3) As the initial energy of the turbulent velocity field increases, the mean bubble radius and dispersion of radii decrease and the concentration of bubbles increases.

4) As the initial length scale of the turbulent velocity field increases, the mean bubble radius and the dispersion of the function $f_1(r)$ increase, and the concentration of bubbles decreases.

5) As volume gas content in the flow increases, the final values of the mean bubble radius, dispersion of the distribution of $f_1(r)$, and concentration of bubbles per unit volume increase.

Thus, the distribution of probabilities of radii and concentration of bubbles in a turbulent gas-liquid flow can be effectively controlled by varying the initial energy, the initial scale of the length of turbulent fluctuations of liquid, and the volume gas content.

The work was carried out with financial support from the Fundamental Research Fund of the Republic of Belarus.

NOTATION

$f_1(r)$, probability density of bubble radius size; $P_t(r)$, turbulent energy distribution over different length scales; a_{cr} , critical bubble radius; Re , Reynolds number of turbulent flow; We , Weber number; $\omega(r, R)$, functions describing mode of fractionation of bubbles of radius R to bubbles of radius r ; σ , surface tension coefficient; $\tau(r)$, characteristic time of bubble fractionation; L , initial macroscale of velocity fluctuation field; $B(0)$ initial energy of turbulent flow; $\bar{r}(t)$, time-varying mean radius of bubbles; Δ , half-width of initial distribution of $f_0(r)$; ρ' , gas density; ρ , liquid density. Subscripts: t, time; c, characteristic value.

REFERENCES

1. V. A. Sosinovich, V. A. Tsyganov, B. A. Kolovandin, B. I. Puris, and V. A. Gertsovich, *Inzh.-Fiz. Zh.*, **68**, No. 2, 192-204 (1995).
2. V. M. Voloshchuk and Yu. S. Sedunov, *Coagulation Processes in Disperse Systems* [in Russian], Leningrad (1975).
3. V. A. Sosinovich, V. A. Tsyganov, B. A. Kolovandin, B. I. Puris, and V. A. Gertsovich, *Mathematical model of bubble splitting and coalescence in liquid flow*. Preprint No. 6 of the Academic Scientific Complex "A. V. Luikov Heat and Mass Transfer Institute of the Academy of Sciences of the Republic of Belarus" (1994).
4. V. G. Levich, *Physicochemical Hydrodynamics* [in Russian], Moscow (1959).
5. S. Chandrasekhar, *Stochastic Problems in Physics and Astronomy* [Russian translation], Moscow (1942).
6. V. A. Sosinovich, B. A. Kolovandin, V. A. Tsyganov, and C. Meola, *Int. J. Heat Mass Transfer*, **30**, No. 3, 517-526 (1987).
7. V. S. Fedotovskii and V. P. Bobkov, *Inzh.-Fiz. Zh.*, **31**, No. 4, 678-683 (1976).
8. G. Birkhof, *Hydrodynamics* [in Russian], Moscow (1963).
9. R. I. Nigmatulin, *Dynamics of Multiphase Media*, Pt. 1 [in Russian], Moscow (1987).